

# Mayr's Equation-Based Model for Pantograph Arc of High-Speed Railway Traction System

Yu-Jen Liu, *Student Member, IEEE*, Gary W. Chang, *Senior Member, IEEE*, and Hunter M. Huang, *Member, IEEE*

**Abstract**—This letter presents an extended Mayr's equation-based model for the pantograph detachment arc of the high-speed railway traction system. The proposed model is composed of Mayr's model for arc behavior control and time-controlled switches for starting pantograph detachment and re-attachment events, which are developed by MODELS language and TACS in EMTP/ATP. With the combination of traction motor drive circuit, an effective simulation is performed to observe harmonic spectrum of pantograph current that caused by pantograph detachment arcs. By comparing with the actual measurements for validation, it shows that the proposed arc model is useful for estimating the harmonic frequency range of the pantograph arc current and for power quality studies.

**Index Terms**—Mayr's arc model, pantograph, harmonics, EMI, traction motor drive

## I. INTRODUCTION

WITH the advanced development of railway and power-electronic technologies, the high-speed railway becomes more popular and some power quality problems may be imposed on the supply system and the surrounding environment. One of the main problems in high-speed train systems is to counteract the fast variations of detachments of the contact between the overhead catenary system (OCS) line and the pantograph collector. Such detachments will generate electric arcs that produce a wide range of harmonics. The arcs also may damage the mechanical structure that compromises the collection of the current from the supply wire. When the pantograph detachment occurs in a high-speed train, the arc current generates significant low- and high-frequency current components because of the arc nonlinearity. For the AC traction system, the detachment of pantograph is a dynamic arc behavior and is highly dependent on the arc power loss, the point on the voltage wave, the arc time constant, and the arc conductance. The purpose of this letter tries to propose an effective dynamic arc model to study arc current behavior due to the pantograph detachment.

## II. MODELING PANTOGRAPH DETACHMENT ARC

Typically the high-speed railway traction system includes a single-phase electrified AC railway system that fed by the traction substations. The power is supplied by AC/DC phase-controlled thyristor converters to feed the three-level interlaced pulse-width-modulated (PWM) controlled ac motor drives [1]. At the train pantograph, the harmonic current of the traction drive and the harmonic impedance intact which cause line voltage distortion and consequently conducted high-frequency emissions along the line [2]. The losing mechanical contact between the pantograph and the overhead wire

generates an electric arc. Usually, the arc does not extinguish during normal operations and the current remains due to the inductance of the traction drive system.

The pantograph detachment causes electromagnetic transients to the railway traction drive. Therefore, the pantograph detachment can be modeled by an arc resistance and two time-controlled switching devices for the established and extinguished arcs. Figure 1 shows the equivalent circuit of the traction system with considering pantograph arc behavior, where the pantograph detachment arc occurred on the railway OCS is modeled by the Mayr's arc model. The arc conductance,  $G_{arc}$ , is assumed to be a large value when the arc is produced and a small value when the arc is extinguished. Two switches,  $SW_0$  and  $SW_C$ , are used to determine the pantograph detachment and re-attachment.

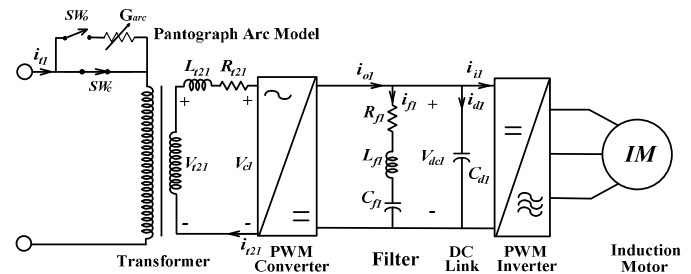


Fig. 1. Equivalent circuit of the high-speed railway traction drive including the pantograph arc model.

The Mayr's equation of (1) is commonly used in modeling arcs for transient studies with considering circuit interactions, thermal behaviors, resonant oscillations, and arc instability, where  $G_{arc}$  is arc conductance,  $\theta$  is arc time constant, and  $N_0$  is the arc power loss [3]. The proposed model based on (1) permits observing the high-frequency current components caused by the pantograph detachment. Figure 2 depicts the schematic diagram of the proposed arc model for simulations, where the Mayr's arc equation is implemented in the MODEL block, the initial value of  $G_{arc}$ , the parameters  $\theta$ ,  $i_{arc}$ , and  $N_0$  are required as input into Mayr's equation to solve (1).

$$\frac{dG_{arc}}{dt} = \frac{G_{arc}}{\theta} \left[ \frac{i_{arc}^2}{N_0} - G_{arc} \right] \quad (1)$$

The MODEL block includes the EMTP TACS control combined with Mayr's equation of (1), where the on/off states of the  $SW_C$ , and the arc current,  $i_{arc}(t)$  representing pantograph detachment conditions are input to MODEL. The arc conductance,  $G_{arc}(t)$ , is then calculated and output to decide the TACS  $SW_0$  (i.e. detachment) state. At the instant of  $SW_C$  opening, MODEL starts the arc event and controls the changing rate of the arc conductance at every simulated time step by using the input parameters. If the current is chopped, it implies that the arc conductance is lower than the minimum setting value or the gap detachment arcing time is longer than

This work was supported by National Science Council of Taiwan, R.O.C. under grants NSC 95-2221-E-194-100-MY3 and NSC 96-2213-E-194-056.

The authors are with the Department of Electrical Engineering, National Chung Cheng University, Taiwan, R.O.C. (e-mail: wchang@ee.ccu.edu.tw).

the predicted one or the air gap withstands a voltage of pantograph detachment being higher than the maximum transient arc voltage, then TACS  $SW_0$  is opened and the arc thermodynamic control is completed. The initial arc power loss depends on the capacitance and voltage difference between the pantograph and the OCS, which is determined by the pantograph detachment gap and the surrounding air. The total arc energy depends on the total arc time from the detachment to the reattached time of the pantograph and the train speed. The arc time constant,  $\theta$ , is highly dominated by the thermal inertia of the arc and the arc instability frequency. In practice, the values of these parameters can be obtained by laboratory or field measurements, or by numerical experiences. The parameters are then used to solve (1).

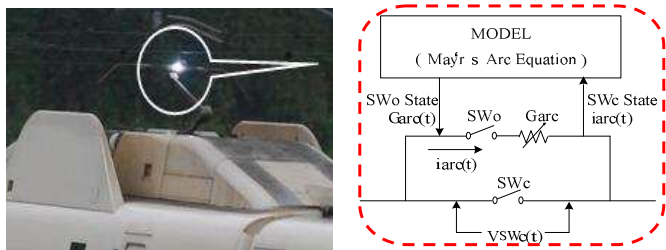


Fig. 2. Schematic diagram of the proposed pantograph detachment arc model for SKS-700T high-speed railway train.

### III. ACTUAL MEASUREMENTS AND SIMULATION RESULTS

A 10-km feeder of 25kV OCS fed by a substation is modeled by a number of 500-meter equivalent  $\pi$  circuits. Simulations are performed by using EMTP/ATP, where the train is assumed to be located at the middle of the feeder running at full load. Parameters of the traction system required for simulations are listed in Table I. In field measurements, the arc signals near the pantograph received from the digital antenna are picked up by an equipped digital storage oscilloscope. Figure 3 shows the measured and simulated the pantograph arc current waveforms. Figure 4 illustrates the frequency spectra obtained by FFT of Fig. 3 under a sampling rate of 20 MHz. By observing the spectra of Fig. 4, it is found that the 5-th harmonic is dominant in the low-frequency range and those components within 1 MHz produced are mainly because of the switching operations of the PWM-type traction motor drive and can be regarded as sources of conductive EMI to neighboring circuits.

### IV. CONCLUSIONS

This letter has proposed an extended Mayr's equation-based arc model to effectively observe the pantograph arc behavior. Through the FFT analysis of the pantograph arc current, it shows that the pantograph arc behavior contributes a wide range of harmonic components. The low- to high-frequency harmonic components of the arc current present as sources of power quality disturbances. Future work will focus on accurately measuring arc parameters for the proposed model and improving the solution accuracy.

### V. REFERENCES

- [1] G. W. Chang, H. W. Lin, and S. K. Chen, "Modeling characteristics of harmonic currents generated by high-speed railway traction drive

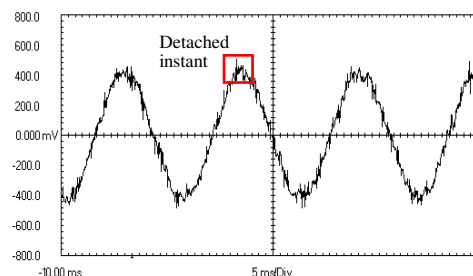
converters," *IEEE Trans. on Power Delivery*, vol. 19, no. 2, April 2004, pp. 766-773.

- [2] A. Mariscotti and P. Pozzobon, "Synthesis of line impedance expressions for railway traction systems," *IEEE Trans. on Vehicular Technology*, vol. 52, no. 2, March 2003, pp. 420-430.
- [3] "Applications of black box modelling to circuit breakers," *Electra*, no. 149, pp. 41-71, Aug. 1993.

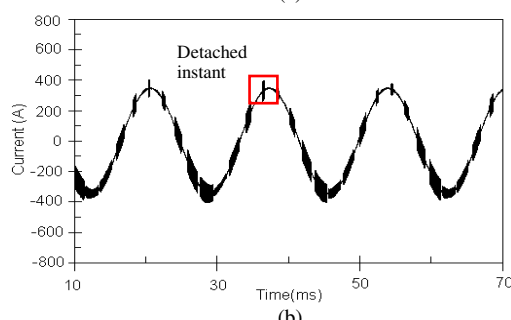
TABLE I: PARAMETERS OF SIMULATED TRACTION CIRCUIT IN FIG. 1

Arc Model Input	$G_{arc0} = 47.74$ mho, $\theta = 0.16$ $\mu$ s, $N_0 = 156.48$ W
Transformer	$V_{t1} = 25$ kV, $V_{t2} = 1.45$ kV, $P_{t2} = 8.4$ MW @60 Hz, $X_{pu} = 0.34$ p.u., $L_t = 1.75$ mH, $R_t = 0.01357$ $\Omega$
PWM Converter	$M_R = 9$ , $M_a = 0.8$
Filter	$R_f = 15$ m $\Omega$ , $L_f = 0.7033$ mH, $C_f = 2.5$ mF
DC Link	$C_{d1} = 5$ mF, $C_{d2} = 5$ mF
PWM Inverter	$M_R = 25$ , $M_a = 0.95$
Induction Motor	Rated Input Power = 285 kW

$M_R$ : ratio of the carrier frequency to the modulation one;  $M_a$ : the modulation index

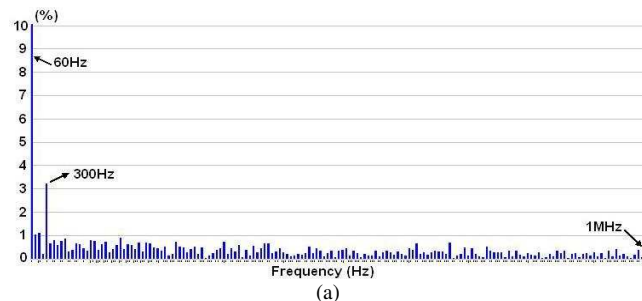


(a)

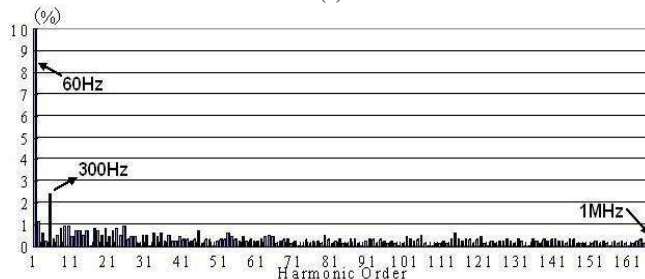


(b)

Fig. 3. Pantograph arc current waveforms: (a) measured (1mV/1A), (b) simulated.



(a)



(b)

Fig. 4. Frequency spectra of pantograph arc current: (a) measured, (b) simulated.